Supplement of Biogeosciences, 21, 3075–3091, 2024
https://doi.org/10.5194/bg-21-3075-2024-supplement

Biogeosciences Open Access EGU

Supplement of

Vegetation patterns associated with nutrient availability and supply in high-elevation tropical Andean ecosystems

Armando Molina et al.

Correspondence to: Armando Molina (armando.molinav@ucuenca.edu.ec) and Veerle Vanacker (veerle.vanacker@uclouvain.be)

Table S1: Mean annual volumetric water content, and the effective and maximum rooting depth per soil profile.

	VMC	Rooting depth (cm)	
	$cm^3\ cm^{-3}$	Effective roots	Maximum rooting
FR1 Upper	0.55	no data	no data
FR1 Middle	0.49	no data	no data
FR1 Lower	0.50	no data	no data
FR2 Upper	0.55	35	80
FR2 Middle	0.49	45	60
FR2 Lower	0.49	55	85
FR3 Upper	0.55	45	65
FR3 Middle	0.49	40	90
FR3 Lower	0.50	45	110
PR1 Upper	0.55	25	no data
PR1 Middle	0.49	30	80
PR1 Lower	0.53	35	60
PR2 Upper	0.57	42	100
PR2 Middle	0.60	50	100
PR2 Lower	0.53	50	90
PR3 Upper	0.60	50	70
PR3 Middle	0.65	45	65
PR3 Lower	0.58	35	50
PR4 Upper	0.60	35	55
PR4 Middle	0.62	50	100
PR4 Lower	0.55	45	85
PR5 Upper	0.56	40	65
PR5 Middle	0.50	40	70
PR5 Lower	0.55	40	60
CU2 Upper	0.51	35	60
CU2 Middle	0.71	30	45
CU2 Lower	0.57	30	70
CU3 Upper	0.51	40	40
CU3 Middle	0.73	40	50
CU3 Lower	0.59	35	45
CU4 Upper	0.54	30	50
CU4 Middle	0.73	30	50
CU4 Lower	0.61	31	50
Mean ± 1 SD			
Forest (FR)	0.51±0.03	44±6	82±16
Tussock grasses (PR)	0.57±0.04	41±8	75±17
Cushion plants (CU)	0.61±0.08	33±4	51±8

Table S2 : Saturated hydraulic conductivity (mm h^{-1}) of the 12 selected soil profiles. The hydraulic conductivity was measured using the inverse auger hole method, and the reported values are the mean values of three replicates.

	Horizon	Hydraulic conductivity mm h^{-1}
FR3 Upper	A	6.0
	C	0.3
FR3 Middle	A	9.3
	C	5.6
FR3 Lower	A	7.7
	C	6.8
PR3 Upper	A	6.1
	C	NA
PR3 Middle	A	2.6
	C	4.9
PR3 Lower	A	2.9
	C	0.4
PR5 Upper	A	2.3
	C	1.8
PR5 Middle	A	2.5
	C	1.0
PR5 Lower	A	4.6
	C	3.3
CU4 Upper	A	5.0
	C	0.5
CU4 Middle	A	1.4
	C	0.0
CU4 Lower	A	11.9
	C	0.0

Table S3 : Soil hydrological parameters of 12 selected soil profiles derived from the chloride concentrations in rain and soil water using the approach of White et al. (2009) and Buss et al. (2017).

	Precip. Cl µM	Soil water Cl µM	Precip. flux q_{preci} m yr^{-1}	Soil water flux, q_h m yr^{-1}	Porosity Ø m^3 m^{-3}	Saturation ſ m^3 m^{-3}	Infiltration Rate m yr^{-1}	Residence time yr
Rainfall	13		0.55					
FR3 Upper		17		0.43	0.70	0.65		
FR3 Middle		19		0.38	0.73	0.56		
FR3 Lower		19		0.39	0.66	0.70		
PR3 Upper		15		0.51	0.75	0.77		
PR3 Middle		12		0.59	0.79	0.76		
PR3 Lower		13		0.58	0.71	0.72		
PR5 Upper		49		0.15	0.65	0.63		
PR5 Middle		18		0.40	0.72	0.69		
PR5 Lower		14		0.54	0.71	0.69		
CU4 Upper		17		0.43	0.57	0.71		
CU4 Middle		24		0.31	0.64	0.76		
CU4 Lower		25		0.30	0.65	0.65		
Mean ±1 SD								
FR				0.40±0.03	0.70±0.03	0.64±0.07	***0.90***	***0.55***
PR				0.46±0.17	0.72±0.05	0.71±0.05	***0.91***	***0.55***
CU				0.35±0.08	0.62±0.04	0.71±0.05	***0.79***	***0.63***

Table S4: Mean (± 1 SD) annual ion concentrations (µM) and pH of the soil solutes per soil profile.

	Ca	K	Mg	Na	Si	P	Cl	S	Al	Fe	pH
			µM								
FR1 Upper	15±9	27±36	7±8	32±19	6±3	0.1±0.1	17±19	7±3	16±7	1±0	5.6±0.4
FR1 Lower	19±5	95±10	8±3	33±19	9±10	0.2±0.1	21±8	17±2	12±6	1±0	5.8±0.3
FR2 Upper	40±44	22±33	17±23	173±55	14±10	0.4±0.2	28±25	14±5	21±22	1±1	5.6±0.5
FR2 Middle	21±6	19±17	12±3	89±17	68±53	0.2±0.1	15±6	10±12	2±2	1±2	6.7±0.2
FR2 Lower	17±8	22±15	12±7	50±12	10±7	0.2±0.1	18±11	9±1	11±9	1±0	5.6±0.3
FR3 Middle	63±14	57±14	28±8	45±19	10±7	0.2±0.2	19±11	6±1	23±11	1±0	4.9±0.5
FR3 Lower	19±4	27±3	10±2	62±15	12±9	0.1±0.1	19±7	15±1	3±3	1±0	6.3±0.2
PR1 Upper	22±5	23±4	11±4	82±26	44±42	0.4±0.5	13±9	4±2	3±3	3±8	6.6±0.2
PR1 Middle	26±11	8±4	9±4	69±27	43±31	0.4±0.2	16±8	5±4	1±1	0.2±0.1	6.6±0.3
PR1 Lower	23±5	5±1	12±3	56±11	56±29	0.3±0.3	12±6	2±2	0±1	0.2±0.2	6.6±0.3
PR2 Upper	10±4	4±2	6±3	51±17	22±42	0.2±0.2	9±2	2±1	1±1	0.2±0.2	6.4±0.2
PR2 Middle	10±3	5±3	5±3	28±15	21±44	0.2±0.1	8±7	2±2	1±1	0.3±0.2	6.3±0.2
PR2 Lower	16±5	6±1	9±3	35±19	19±20	0.1±0.1	10±5	2±1	2±2	0.4±0.3	6.5±0.2
PR3 Upper	14±2	18±3	6±2	52±15	14±10	0.1±0.1	15±7	3±1	3±3	6±7	6.4±0.2
PR3 Middle	17±3	15±6	9±3	27±14	8±7	0.2±0.2	12±6	4±3	4±3	2±2	6.3±0.3
PR3 Lower	23±6	8±3	12±3	45±14	17±19	0.1±0.1	13±5	6±2	3±3	1±0	6.6±0.2
PR4 Upper	15±5	20±26	7±5	56±27	15±14	0.3±0.4	16±8	5±4	3±3	3±5	6.4±0.2
PR4 Middle	12±5	4±3	5±4	39±24	19±45	0.1±0.1	9±6	2±1	2±2	2±3	6.4±0.2
PR4 Lower	14±4	8±2	5±1	33±16	9±14	0.2±0.1	10±6	4±2	5±3	1±1	6.2±0.3
PR5 Upper	33±10	28±7	13±4	76±29	43±29	0.2±0.1	49±18	6±2	1±1	0.3±0.2	6.6±0.2
PR5 Middle	26±7	5±2	10±4	90±21	100±62	0.2±0.2	18±9	4±2	1±1	0.2±0.1	6.7±0.2
PR5 Lower	29±13	14±5	8±3	136±47	147±81	0.2±0.2	14±6	5±3	1±1	1±1	6.9±0.2
CU2 Upper	60±12	17±3	30±6	104±24	261±62	0.2±0.2	14±9	3±2	1±0	4±4	7.1±0.3
CU2 Middle	56±9	4±2	43±7	97±14	97±74	0.1±0.1	16±7	3±1	1±1	10±13	7.0±0.2
CU2 Lower	38±6	4±2	27±4	105±23	99±76	0.1±0.1	12±8	3±2	1±1	3±6	6.9±0.1
CU3 Upper	92±17	17±2	16±6	177±29	277±161	0.2±0.2	25±12	5±1	2±3	1±1	7.0±0.2
CU3 Middle	85±12	11±1	19±2	162±19	232±111	0.2±0.1	16±5	4±1	1±1	1±1	7.1±0.2
CU3 Lower	93±45	22±27	25±14	211±64	362±122	0.3±0.1	28±30	10±16	2±3	1±1	7.3±0.3
U4 Upper	89±17	23±2	10±3	186±35	427±182	0.1±0.1	17±11	4±1	1±1	0.2±0.1	7.2±0.1
CU4 Middle	162±62	38±5	35±13	355±22	472±168	0.3±0.2	24±10	3±1	1±1	3±4	7.5±0.4
CU4 Lower	66±21	17±4	15±4	230±59	390±193	0.2±0.1	25±24	4±3	2±2	1±1	7.1±0.2

45

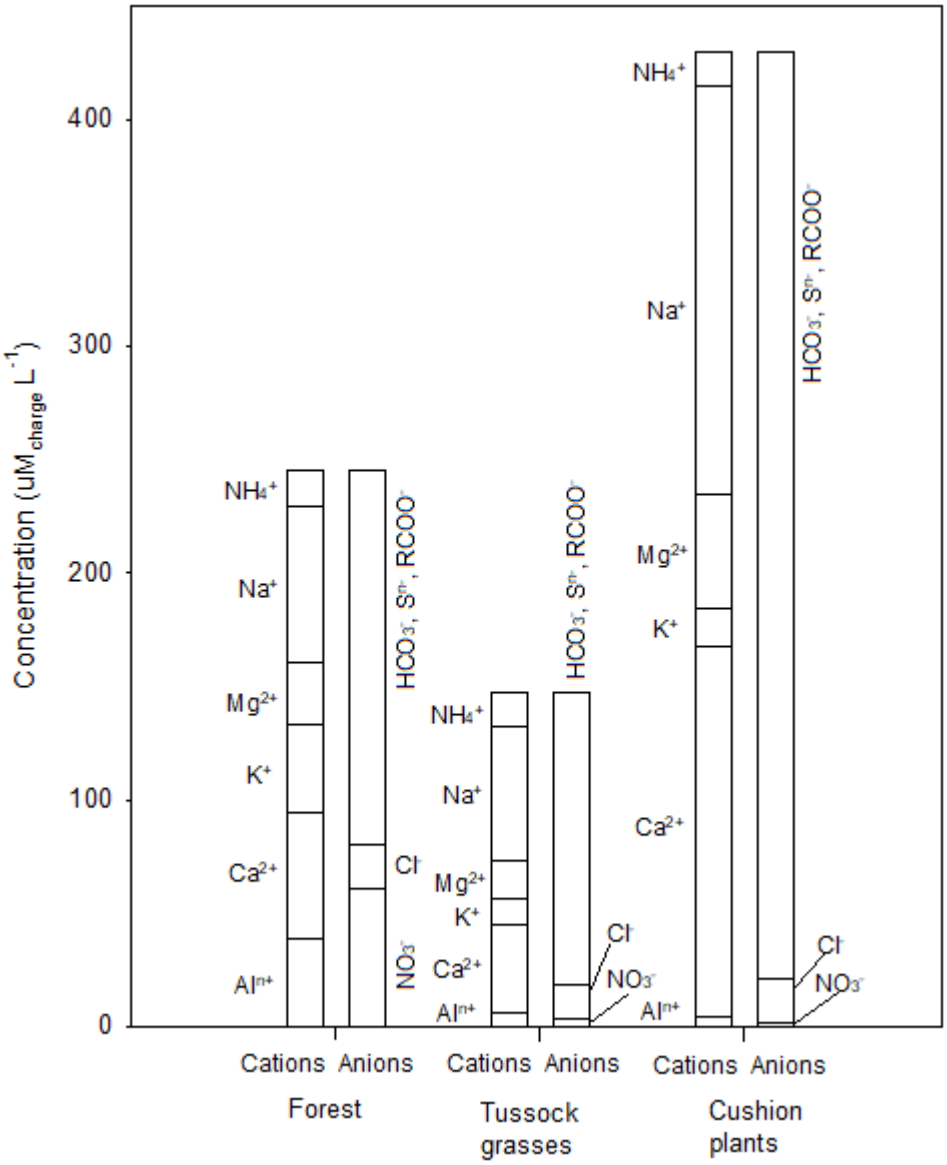

Figure S1: Partial cation–anion charge balance of the major solutes (i.e., those with concentrations > 2 µmol$_c$ L^{-1}) in soil water at a depth of 0.5 m. The X-axis scale shows the three different vegetation types. The contribution of bicarbonates (HCO_3^-) and organic acids ($RCOO^-$) were estimated by subtracting the total anion charge from the total cation charge, whereby the charge contributions of the total Al were assumed to be 3+.

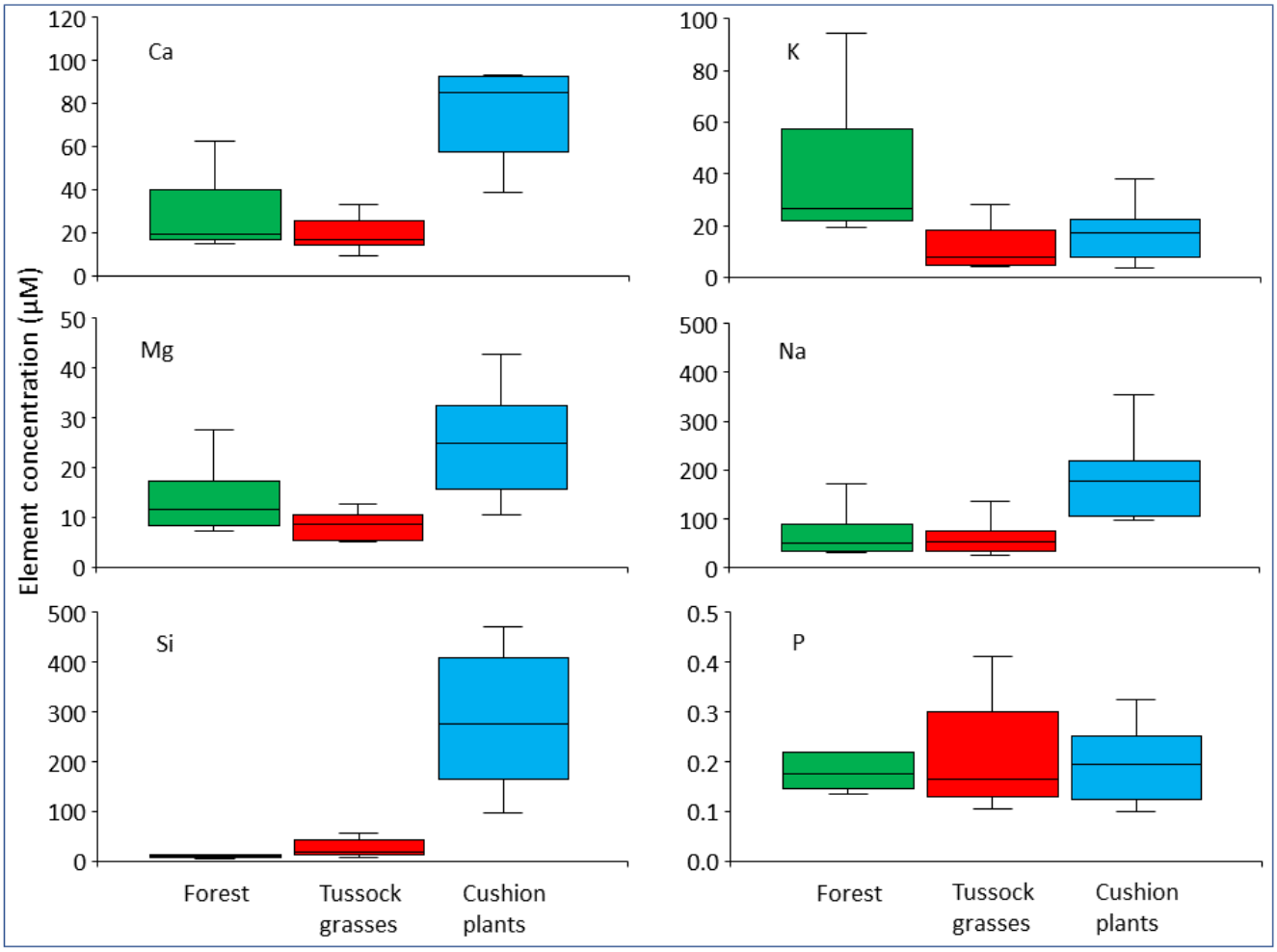

Figure S2: Major element concentrations in soil pore water (µM) under forests (n=7), tussock grasses (n=15) and cushion plants (n=9). The boxplots show the median, the 25th and 75th percentile, and the whiskers the minimum and maximum observed values.

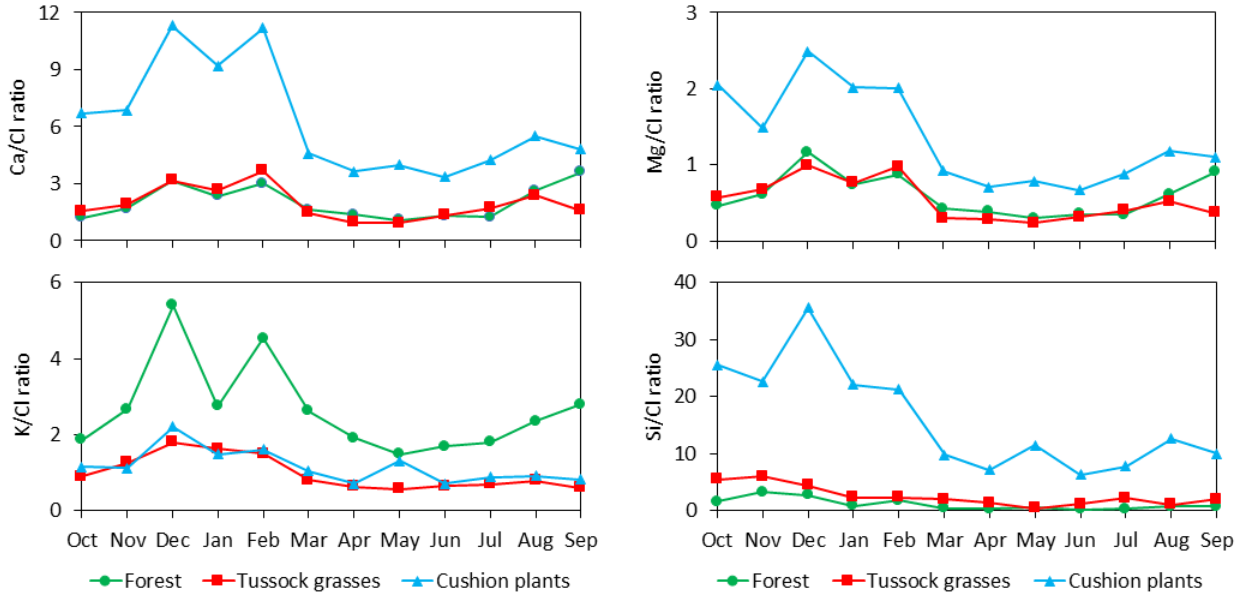

Figure S3: Temporal variation in the ratio of Ca, Mg and K nutrients to Chloride in the soil solutes under forest (n=7), tussock grasses (n=15) and cushion plants (n=9). The mean monthly values were derived from the biweekly measurements in the soil profiles over the period October 2012 till September 2013.

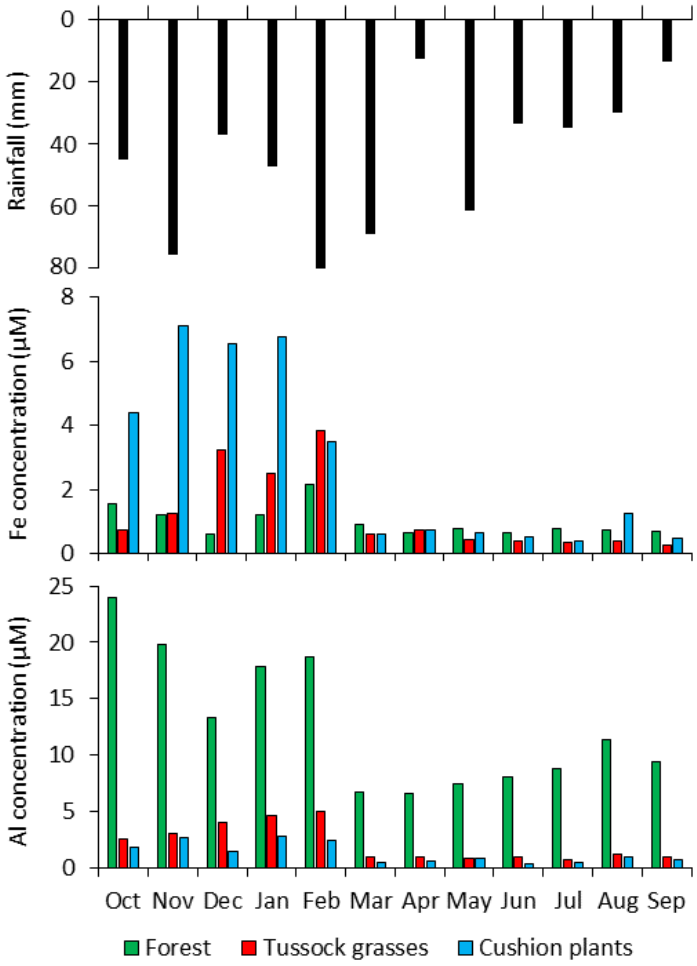

Figure S4: Mean monthly rainfall (mm) and mean monthly Al and Fe concentrations (µM) in soil solutes under forest (n=7), tussock grasses (n=15) and cushion plants (n=9). The mean monthly values were derived from the biweekly measurements in the soil profiles over the period October 2012 till September 2013.

References

Buss, H. L., Chapela Lara, M., Moore, O. W., Kurtz, A. C., Schulz, M. S., and White, A. F.: Lithological influences on contemporary and long-term regolith weathering at the Luquillo Critical Zone Observatory, Geochim. Cosmochim. Ac., 196, 224–251, https://doi.org/10.1016/j.gca.2016.09.038, 2017.

White, A. F., Schulz, M. S., Stonestrom, D. A., Vivit, D. V., Fitzpatrick, J., Bullen, T. D., Maher, K., and Blum, A. E.: Chemical weathering of a marine terrace chronosequence, Santa Cruz, California. Part II: Solute profiles, gradients and the comparisons of contemporary and long-term weathering rates, Geochim. Cosmochim. Acta, 73, 2769–2803, https://doi.org/10.1016/j.gca.2009.01.029, 2009.